A Cutoff in the X-ray Fluctuation Power Density Spectrum of the Seyfert 1 Galaxy NGC 3516

Rick Edelson
X-Ray Astronomy Group; Leicester University; Leicester LE1 7RH; United Kingdom

ABSTRACT

RXTE observed the bright, strongly variable Seyfert 1 galaxy NGC 3516 once every ∼12.8 hr for 4.5 months and nearly continuously for a 4.2 day period in the middle, followed by ongoing monitoring once every ∼4.3 days. These data are used to construct the first well-determined X-ray fluctuation power density spectrum (PDS) of an active galaxy to span more than 4 decades of usable temporal frequency. The PDS shows a progressive flattening of the power-law slope from –1.74 at short time scales to –0.73 at longer time scales, the clearest observation to date of the long-predicted cutoff in the PDS. The characteristic variability time scale is ∼1 month. The PDS appears similar to those seen for Galactic black hole candidates such as Cyg X-1, suggesting that these two classes of objects with very different luminosities and putative black hole masses (differing by more than a factor of 10^5) may have similar X-ray generation processes and structures. This *RXTE* experiment was only possible because of NGC 3516's special placement in the sky allowed quasi-continuous observations. Because of *XMM*'s highly eccentric orbit, it will be possible to combine *XMM* and *RXTE* data will allow similar experiments for objects throughout the sky.

1. Introduction

X-ray variability can, in principle, provide strong constraints on the physical conditions in the centers of Active Galactic Nuclei (AGN). Early observations of rapid variability in Seyfert galaxies implied large luminosity densities, providing the first compelling argument for the standard black hole/accretion disk model (Rees 1984). In some models, the X-ray source is the primary emission component, so X-ray variability may be the most direct way to probe the smallest accessible regions of the central engine. Measurement of a "characteristic variability time scale" may allow determination of the source size, luminosity density, and black hole mass. Early attempts to do this with unevenly sampled data involved measuring the "e-folding time," but this quantity is unstable, depending strongly on sampling length and signal-to-noise ratio (Press 1978).

The best way to measure the characteristic variability time scale, and to characterize AGN variability in general, is to determine the fluctuation power density spectrum (PDS). Because of its highly eccentric orbit, *EXOSAT* provided the most useful AGN light curves gathered until recently with its uninterrupted 2–3 day "long-looks." The *EXOSAT* long-look PDS had a usable

dynamic range of about 1.7 decades of temporal frequency ($\sim 10^{-3}$ to 2×10^{-5} Hz, or $\sim 10^{3}$ to 5×10^{4} sec). These PDS generally rise smoothly to longer time scales as a power-law ($P(f) \propto f^{a}$, where $P(f)$ is the power at temporal frequency f), with no features or signs of periodicity. All were apparently consistent with a single form, so-called "red noise" because the high temporal frequency slopes were steep ($a \approx -1.5$; Green et al. 1993; Lawrence & Papadakis 1993). A turnover (identified as a characteristic variability time scale) must occur at some longer time scale or the total variability power would diverge, but these PDS were not able to detect it because of the lack of low temporal frequency coverage. Attempts to constrain this cutoff by combining data from a number of unrelated observations (e.g., McHardy 1989, Papadakis & McHardy 1995) required complex and non-standard techniques that were not able to directly determine the PDS. Here we present the results of more standard PDS analysis of a new body of near-evenly sampled data.

2. Observations

It was only after *EXOSAT*'s mission had ended that the importance of evenly-sampled data and simultaneously probing long and short time scales became apparent. All X-ray satellites launched since then have had low-Earth orbits, for which Earth occultation generally corrupted short-term light curves beyond recovery. However, even though it too had a low-Earth orbit, the launch of the *Rossi X-ray Timing Explorer* (*RXTE*) opened up interesting, new possibilities. It's high throughput, fast slewing and flexible scheduling make it ideal for obtaining even sampling on long time scales. Most importantly for this project, it has a large "continuous viewing zone," defined as a region of sky near the orbital pole for which a source is visible over a number of consecutive orbits without interruption due to Earth occultation.

2.1. NGC 3516

We searched this region of sky and found, by fortunate coincidence, that it contained NGC 3516, a bright ($B \approx 13$) object that was one of the original Seyfert galaxies (Seyfert 1943). It is bright and highly variable in the X-rays as well, with $F(2-10 \text{ keV}) \approx 1.3 - 8 \times 10^{-11}$ erg cm^{-2} sec $^{-1}$ (Ghosh & Soundararjaperumal 1991; Kolman et al. 1993; Kriss et al. 1993; Nandra et al. 1997a). Because it is so bright an strongly variable, and most importantly because of its favorable location in the sky, NGC 3516 was chosen for this experiment.

2.2. Sampling Pattern

The sampling was optimized to obtain variability information spanning time scales from minutes to months. NGC 3516 was observed once every ∼12.8 hr (=8 orbits) for 124 epochs, then quasi-continuously for 4.2 days, then again once every ∼12.8 hr for another 124 epochs. (Combining

the periodic sampling with snippets from the continuous period yielded 256 nearly-evenly-sampled scheduled epochs.) These were followed immediately by observations once every ∼4.3 days (=64 orbits) that are planned to continue for the lifetime of the satellite.

The goal was for the sampling to be as close as possible to strictly periodic on each of three progressively shorter and more densely sampled time scales. This experiment came much closer than any previous effort, although certain unavoidable perturbations must be noted. During the continuous sampling, the light curve was interrupted by SAA passage, and a few time-critical observations of other sources causing a total of 69 ksec (19%) of the data to be lost. The 12.8 hr sampling was interrupted three times for a total of 10 epochs (4%), and the 4.3 day sampling had a total of 3 interruptions (2%). The mean deviation between the ephemeris and observation times was 0.36 hr (2.8% of a fundamental cycle) for the medium time scale and 0.98 hr (1.0%) for the long time scale sampling. (The short time scale data were by definition tied to the ephemeris with no deviation.)

3. Data

3.1. Data Reduction

The *RXTE* Proportional Counter Array (PCA) consists of 5 collimated Proportional Counter Units (PCUs; Jahoda et al. 1996). Our anlaysis was restricted to PCA `STANDARD-2` 2–10 keV top layer dta for PCUs 0, 1 and 2 because this is where the PCA is most sensitive and the systematic errors are best quantified. The data reduction methods employed here are similar to those described by Nandra et al. (1998). Binned light curves were initially extracted with 16 sec time resolution using the criteria that: the Earth elevation angle was greater than 5 degree; the offset between the pointing position and the optical position of NGC 3516 was less than 0.01 degree and to exclude periods where the anti-coincidence rate in the propane layer of the PCUs was abnormal. The 16 sec sampled data were then rebinned to longer sampling intervals as discussed below. The light curve is shown in Figure 1.

Background estimation represents the largest uncertainty for relatively weak sources such as NGC 3516. These data were analyzed with the "`L7`" model, which employs PCA event rates directly related to both the particle and activation rates by a scaling factor, leaving a residual induced term that is modeled as an exponential decay with an e-folding time of 240 min, the amplitude of which is determined by integrating the rates from HEXTE particle monitors. We used offset data taken after the snapshots of NGC 3516 in a region close by, but believed free of bright sources. These offset data were used to assess the systematic errors in the background subtraction, as shown at the bottom of the top panel in Figure 1. The mean is non-zero and the variance is larger than would be expected from statistical fluctuations. The mean and excess deviation are 0.87 and 0.39 c/s, respectively. The corresponding section of the NGC 3516 light curve has an RMS deviation of 4.4 c/s. The ratio of the (variances) is ∼125, meaning that (in

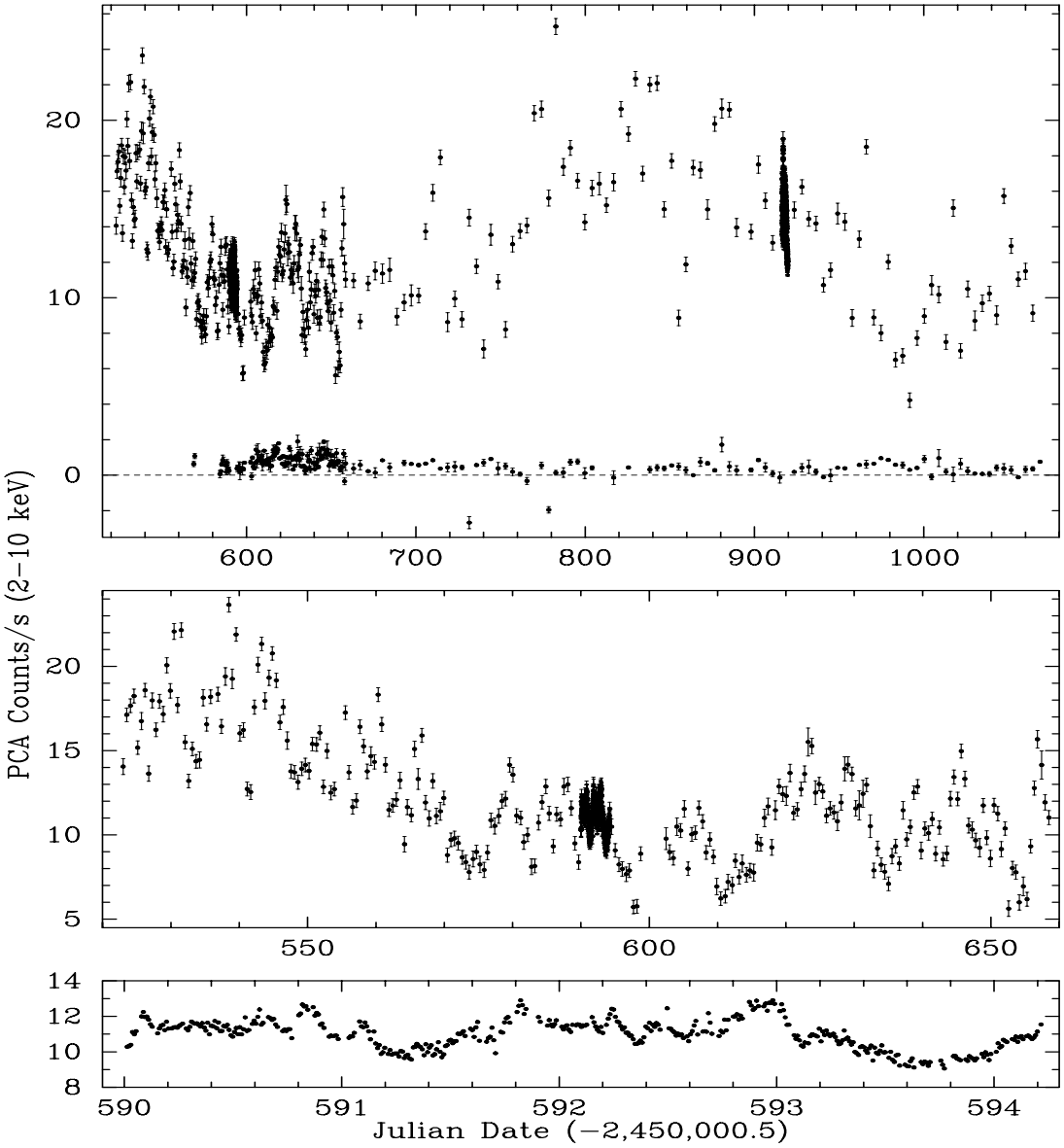

Fig. 1.— *RXTE* light curve of NGC 3516. The top panel covers the period 1997 March 16–1998 September 12. Starting on 1997 July 31, the light curve was sampled every ∼4.3 days. The data at the top is the source light curve while those at the bottom (–1 to +2 c/s) are off-source (background pointings). The middle panel covers the period 1997 March 16 to July 30, during which time observations were made every ∼12.8 hr. The bottom panel shows the data during 1997 May 22 00:01–May 26 05:37, during which time the source was observed quasi-continuously, binned every 710 sec. The abscissa is the background-subtracted PCA 2–10 keV L1 count rate. The error bars are a combination of statistical and systematic uncertainties in the background subtraction. No error bars are shown for the short time scale data because they would make the figure too crowded. However, they are generally the same as in the upper two panels.

the worse case) less than 1% of the observed variability power is due to errors in the background model. We therefore interpret the data under the assumption that the observed variability is dominated by intrinsic changes in the flux of NGC 3516.

3.2. Data Analysis

The measurement of the PDS took two steps: First, the short, medium, and long time scale data were each separately made suitable for analysis and the individual PDS were measured, and then the separate PDS were combined to produce a single PDS.

The uneven sampling that made it so difficult for previous campaigns to estimate the PDS was much less of a problem here. The data were linearly interpolated across the relatively rare data gaps, to produce three light curves: (1) 512 points sampled every 11.8 min, (2) 256 points sampled once every 12.8 hr, and (3) 128 points sampled once every 4.3 days. Because the departures from the ephemeris were almost always small (typically only a few percent), the ephemeris times and not the actual times were used in the analysis, with no interpolation.

PDS were then derived using standard methods from Numerical Recipes (Press et al. 1992) and the logarithms of both frequency and power were taken. The zero-power and next two lowest-frequency points of each PDS were ignored in the further analyses because they tend to be extremely noisy (see Press 1978 for details). The remaining points were binned every factor of two (0.3 in the logarithm), to reduce the noise and allow estimation of error bars. That means that the first binned point was derived by binning the two remaining lowest frequency points, the second by binning the next four points, etc. The PDS were then calculated using a Bartlett window function, $w_j = 1 - \left| \frac{j - \frac{1}{2}N}{\frac{1}{2}N} \right|$. (We also tried square, Welch and Hann window funcions, with no significant changes to the overall results.) Power-law models were fitted to each PDS to estimate the slope.

The results for each light curve are summarized in Table 1: column 2 gives the sampling period, column 3, the number of points, column 4, the range of temporal frequencies sampled, column 5 the slope (and uncertainty) of unweighted, least-squares fits to the each of the logarithmically binned PDS, and column 6, the fractional variability (F_{var}), uncorrected for measurement errors.

The short, medium, and long time scale PDS were then combined to form a single PDS spanning four decades of usable temporal frequency. As shown in Table 1, the PDS shows a highly significant (8σ) systematic flattening from $a = -1.74 \pm 0.12$ to -0.73 ± 0.12 as one goes from short to long time scales.

Thus, a more complex model than a single power-law was required to describe the PDS. All three PDS were combined and simultaneously fitted with a model of a power-law that dominates at high frequencies, but cuts off to a slope of $a = 0$ at very low temporal frequencies. We used the

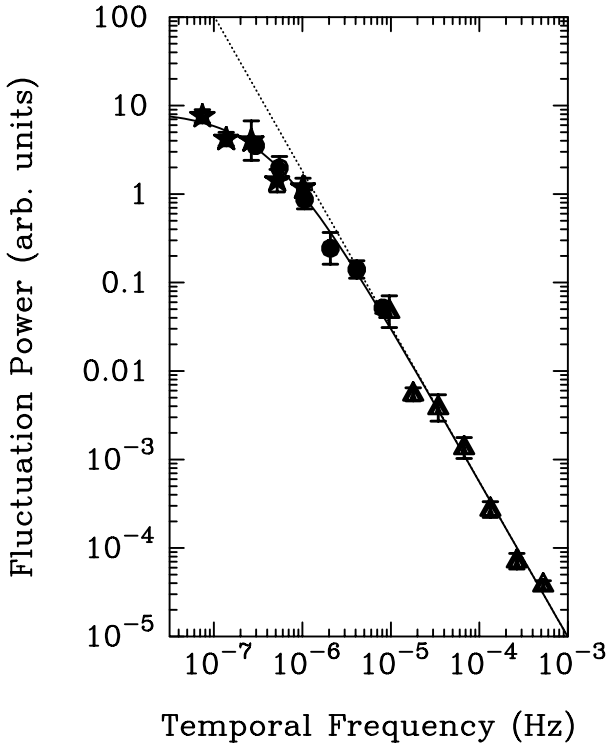

Fig. 2.— Broadband PDS of NGC 3516. The individual PDS in Fig. 2 were combined, scaled and fitted Simultaneously, as described in the text. The plot symbols follow the convention in Fig. 2. The PDS is not consistent with a single power-law; instead it had to be fitted by a power-law that flattened to low frequencies in order to obtain a reasonable fit. This yielded a cutoff frequency of $\sim 4 \times 10^{-7}$ Hz, corresponding to $\sim$1 month.

Table 1. NGC 3516 Campaign Sampling and Variability Parameters

Time Scale	Sampling Interval	Number of Points	Temp. Freq. Range (Hz)	Power-Law Slope (a)	Fractional Variability (F_{var})
Short	11.8 min	512	$5.7 \times 10^{-6} - 7.0 \times 10^{-4}$	-1.74 ± 0.12	7.9%
Medium	12.8 hr	256	$1.7 \times 10^{-7} - 1.1 \times 10^{-5}$	-1.03 ± 0.06	30.1%
Long	4.3 days	128	$4.2 \times 10^{-8} - 1.3 \times 10^{-6}$	-0.73 ± 0.12	31.6%

function

$$P(f) = C/(1 + f/f_c)^a, \quad (1)$$

where $P(f)$ is the fluctuation power at temporal frequency f, a is the power-law slope at high temporal frequencies, f_c is the "cutoff frequency," well below which the PDS flattens to a slope of zero, and C is the normalization. Arbitrary, free *relative* normalizations were allowed between the three individual PDS. The fit was performed by minimizing the Whittle negative log likelihood function with the result shown in Figure 2. The high-frequency slope is $a = -1.76$, similar to the slope derived using the high-frequency PDS alone. The cutoff frequency $f_c = 4.1 \times 10^{-7}$ Hz, corresponding to a time scale of 27 days.

Although it is clear that the PDS is not consistent with a single power-law, the exact shape of the turnover is not well-constrained and the low-frequency behavior is undetermined. The fit assumed $a \to 0$ for $f \ll f_c$, but in fact it could be any slope with $a > -1$. (For $a \leq -1$, the total variability power would diverge.)

Finally, the F_{var} values in Table 2 give independent evidence for a cutoff in the PDS at the longest time scales sampled. F_{var} rises from 7.9% to 30.1% for short and medium time scale data taken over a period of 4.2 days and 4.5 months, respectively. However, it shows little further rise in the long time scale data, flattening out to 31.6% for sampling over 1.5 years. Again, visual examination of Figure 1 also indicates that there is very little extra variability power on the longest time scales sampled.

4. Discussion

We have utilized near-evenly sampled light curves of NGC 3516 over an unprecedented range of time scales to construct a PDS over 4 decades of temporal frequency. On short time scales, NGC 3516 exhibits "red-noise" with a high-frequency slope of $a = -1.76$. The PDS is seen to progressively flatten at longer time scales and determining the variability time scale from these data is difficult, but our best estimate is $t_c \approx 1$ month.

4.1. Light Crossing Time

The observed cutoff should be related to the fundamental physics that generates the variability. The fastest possible variability time scale for a coherent, isotropically-emitting region is the light-crossing time ($t_{\rm lc} = 0.011\ (M_{BH}/10^7 M_\odot)\ (R/10R_S)$ day). Here M_{BH} is the black hole mass, R is the distance from the center of mass and R_S is the Schwarzschild radius. The likely black hole mass for NGC 3516 is in the range $10^7 - 10^8$ $M_\odot$, considering its luminosity. This implies that $t_{\rm lc}$ is orders of magnitude shorter than the turnover time scale $t_{\rm c}$. An even more compelling argument against the light-crossing time is that reverberation mapping indicates that

the (optical) broad emission line region in NGC 3516 is light-days to light-weeks across (Wanders et al. 1993), again smaller than the continuum source under the light-crossing assumption. Finally, the presence of a broad, iron Kα line in NGC 3516 (Nandra et al. 1997a,b) indicates that the X-ray continuum-producing region lies inside the 100 $R_{\rm S}$ within which the bulk of that emission line is produced. We therefore conclude that the turnover cannot be due purely to light-travel time effects in the X-ray source.

4.2. Comptonization

The process by which X-rays are produced in AGN is still not known, but typically models have concentrated on Compton upscattering of ultraviolet "seed" photons that probably arise in an accretion disk (e.g., Haardt & Maraschi 1991, 1993; Zdziarski et al. 1994; Stern et al. 1995). In such a Comptonizing plasma, optical depth effects can smear out the variability, changing the power spectrum. The effect is negligible for low optical depth ($\tau \ll 1$), but for $\tau > 1$ the time scale is increased by approximately τ^2. In such models, the turnover would be identified with the size of the scattering region, modified by optical depth effects. Identification of the observed turnover with such a process would require both a large region and a large optical depth. Even at the limits of plausible parameter space ($M_{BH} \approx 10^8$ M$_\odot$ and $R \approx 100 R_{\rm S}$, however, an optical depth of order $\tau \sim 10$ would be required to match the observed value of $t_{\rm c}$. Current models of the X-ray spectra of AGN usually assume lower optical depths, and in fact most are optically thin (Haardt & Maraschi 1991, 1993; Stern et al. 1995; Zdziarski et al. 1995), although some have optical depths as large as a few (e.g., Titarchuk & Mastichidias 1994), so this mechanism is not plausable.

4.3. Other Time Scales

Other relevant time scales are, from Kepler's Third Law, the matter orbital time scale ($t_{\rm orb} = 0.33\ (M_{BH}/10^7 M_\odot)\ (R/10R_S)^{3/2}$ day), and for an accretion disk, the thermal ($t_{\rm th} = 5.3\ (\alpha/0.01)^{-1}\ (M_{BH}/10^7 M_\odot)\ (R/10R_S)^{3/2}$ day), sound crossing ($t_{\rm sound} = 33\ (R/100H)\ (M_{BH}/10^7 M_\odot)\ (R/10R_S)^{3/2}$ day), and radial drift/viscous time scales ($t_{\rm drift} = 53000\ (R/H)^2\ (\alpha/0.01)^{-1}\ (M_{BH}/10^7 M_\odot)\ (R/10R_S)^{3/2}$ day; Maraschi, Molendi & Stella 1992; Treves, Maraschi & Abramowicz 1988). Here, α is the viscosity parameter of the disk and H is the scale height of the disk.

One specific model that has been proposed to explain the variability, the PDS and the variation of the PDS with luminosity is the so-called "bright spot" model of Bao & Abramowicz (1996). In such a model the relevant turnover time scale could perhaps be identified with the $t_{\rm orb}$, marginally consistent with the observed cutoff for the extremes of parameter space mentioned above if the emission is produced very far out in the disk.

Mineshige et al. (1994a,b) have presented a model in which the central regions of the accretion

disk are in a "self-organized critical" (SOC) state. In their model the central accretion disk exists in a near-critical state; when the mass density exceeds the critical value an "avalanche" of accretion occurs, emitting X-rays. The turnover time scale corresponds to $t_{\rm drift}$ for the largest emitting region. In a smoothly-accreting system, such as Mineshige et al. assume exists beyond the SOC region, $t_{\rm drift}$ is clearly too long to be associated with our turnover time scale. However, in the critical region in which the putative discrete blobs are present, the radial drift time scale can be much shorter, by a factor $\sim H/R$.

4.4. Comparison with Galactic X-Ray Binaries

The PDS of NGC 3516 looks remarkably like that of Cyg X-1 and other Galactic X-ray binaries (XRBs) in the "low" or hard state (see, e.g., Belloni & Hasinger 1990; Miyamoto et al. 1992; van der Klis 1995). These sources exhibit a "red noise" spectrum at high frequencies with slopes a between -1 and -2. As observed in NGC 3516, they flatten to lower frequencies, with $a \approx 0$ and cutoff frequencies of order 0.1 Hz (XRBs can also exhibit a very low-frequency noise component, which shall be ignored for the purposes of this discussion.) The analogy between these sources and NGC 3516 is clear.

A simple prediction would be that the cutoff frequency would scale with physical size and therefore black hole mass, as one would expect, for example, for the light crossing or orbital time scales. In the absence of other specific models, one can relate the ratios of the black hole masses in Cyg X-1 and NGC 3516 by a simple scaling law. The cutoff frequency for Cyg X-1 varies between $f_{\rm c} = 0.04 - 0.4$ Hz (Belloni & Hasinger 1990) while for NGC 3516, it appears to be of order $f_{\rm c} \approx 4 \times 10^{-7}$ Hz. The ratio is $10^5 - 10^6$. The mass of the compact object in Cyg X-1 is thought to be of order $\sim 10\ M_\odot$ by independent arguments (Herrero et al. 1995). Scaling the variability time scale as the mass ($M \propto R_S \propto t_c$) yields a mass of $\sim 10^6 - 10^7\ M_\odot$ for NGC 3516. This is to be compared with the estimates above for the black hole mass, i.e. similar to but perhaps a bit smaller than anticipated. The luminosities of NGC 3516 and Cyg X-1 also scale as their cutoff frequencies, however, implying a similar Eddington ratio in the two cases.

The similarities in the PDS reinforce the idea that similar physical processes may produce the X-rays in AGN and XRBs. The hard power-law in XRBs are thought to arise from Comptonization by hot electrons and of course similar models have been proposed for AGN. (See Van Paradijs 1998 for an excellent review of XRBs.) XRB models may deserve some consideration for AGN too. Along with the broad-band aperiodic variability, XRBs show quasi-periodic oscillations (QPO), pulsations and bursts. These latter properties are more easily related to the parameters of the central source (mass, magnetic field strength, etc.), but unfortunately, their existence in AGN remains controversial.

5. Conclusions and Future Prospects

By taking even sampling of the light curves of NGC 3516 on time scales that ranged from minutes to months, it has been possible to measure the PDS from 4×10^{-8} to 7×10^{-4} Hz, more than twice the logarithmic dynamic range of the previous best obtained by the *EXOSAT* long-looks. The PDS slope changes from $a = -1.74$ at high temporal frequencies to $a = -0.73$ at low temporal frequencies. The data are well-fitted by a high-frequency power-law with a cutoff at $f_c \approx 4 \times 10^{-7}$ Hz ($\sim$1 month).

The observed cutoff time scale is much too long to be associated with the light-crossing time for any reasonable range of source parameters. It is not terribly consistent with the rotating disk model of Bao & Abramowicz (1996) unless the X-rays are produced in the very outer regions of the disk. It could be reconciled with Comptonization in a corona around an accretion disk (e.g., Haardt & Maraschi 1993) if there are substantial optical depths effects (Kazanas et al. 1997). Another suggestion is that it represents the accretion time scale for blobs in a self-organized critical disk (Mineshige et al. 1994). In any event, measurement of the broad PDS and cutoff are basically new observational results, and at this stage, most models have not been developed to make strong predictions about them.

Perhaps the most striking result is the similarity to the PDS of Galactic XRBs. Besides having similar shapes, a direct scaling of mass with cutoff time scale (or luminosity) yields a black hole mass of $\sim 10^6 - 10^7 M_\odot$ for NGC 3516. This may indicate that similar physical processes operate in both types of compact X-ray sources, spanning many orders of magnitude in luminosity. If so, we could hope to apply what has been learned about XRBs to help understand (the more difficult to study) AGN.

Because of *XMM*'s highly eccentric orbit, it will be possible to obtain nearly uninterrupted AGN light curve spanning 40 hours. By combining such continuous *XMM* observations with *RXTE* observations spanning longer time scales, it will be possible to perform this experiment on any AGN in the sky, not just the rare few that (like NGC 3516) happen to lie in the *RXTE* continuous viewing zone. Thus, the launch of *XMM* will allow measurement of the turnovers in a wide variety of AGN, and systematic study of how PDS parameters (cutoff time scale, high frequency slope, presence of QPO, etc.) varies with source properties like luminosity and type of AGN. This could help illuminate the connection between AGN and XRBs and, in turn, the physics underlying the production of energy in compact X-ray sources.

Paul Nandra, Evan Smith, Tess Jaffe, Gail Rorbach, David Brillinger, Keith Jahoda, Simon Vaughan, Alan Smale, Jean Swank, Dave Smith, Mark Dixon and Nick White all made important contributions to this work. RE acknowledges financial support through NASA *RXTE* grant NAG 5-7315 and contract S-92507-Z.

REFERENCES

Bao, G. & Abramowicz, M. 1996, ApJ, 465, 646

Belloni, T. & Hasinger, G. 1990, A&A, 230, 103

Ghosh, K. & Soundararajaperumal, S. 1991, ApJ, 383, 574

Green, A., McHardy, I. & Lehto, H. 1993, MNRAS, 265, 664

Haardt, & Maraschi, L. 1991, ApJ, 380, L51

Haardt, & Maraschi, L. 1993, ApJ, 413, 507

Herrero, A., Kudritzki, R., Gabler, R., Vilchez, J., Gabler, A. 1995, A&A, 297, 556

Jahoda, K., Swank, J., Giles, A., Stark, M., Strohmayer, T., Zhang, W., Morgan, E.H. 1996, EUV, X-ray and Gamma-ray Instrumentation for Space Astronomy VII, O. H. W. Siegmund and M. A. Grummin, Eds., SPIE 2808, p. 59

Kazanas, D., Hua, X.-M., Titarchuk, L. 1997, ApJ, 480, 735

Kriss, G.A., et al. 1993, ApJ, 467, 629

Kolman, M. et al. 1993, ApJ, 403, 592

Lawrence, A. & Papadakis, I. 1993, ApJ, 414, L85

McHardy, I. in "Two Topics in X-ray Astronomy," Eds. H. Hunt & B. Battrick, ESA SP-296 (ESA:Noordwijk), p. 1111

Maraschi, L., Molendi, S. & Stella, L. 1992, MNRAS, 225, 27

Magorrian, J., et al. 1998, AJ, 115, 2285

Mineshige, S., Ouchi, N., Nishimoti, H. 1994, PASJ, 46, 97

Mineshige, S., Takeuchi, M., Nishimoti, H. 1994, ApJ, 435, L125

Miyamoto, S., Kitamoto, S., Iga, S., Negoro, H., Terada, K. 1992, ApJ, 391, 21L

Nandra, K., George, I., Mushotzky, R., Turner, T. J., Yaqoob, T. 1997a, ApJ, 477, 602

Nandra, K., George, I., Mushotzky, R., Turner, T. J., Yaqoob, T. 1997b, MNRAS, 282, L7

Nandra, K., Clavel, J., Edelson, R., George, I., Malkan, M., Mushotzky, R., Peterson, B. & Turner, T. J. 1998, ApJ, 505, 549

Papadakis, I. & McHardy, I. 1995, MNRAS, 273, 923

Press, W. 1978, Comments on Astrophysics, 7, 103

Press, W. et al. 1992, "Numerical Recipes: The Art of Scientific Computing," 2nd Edition, (Cambridge University Press)

Rees, M. 1984, ARA&A, 22, 472

Seyfert, K. 1943, ApJ, 97, 28

Stern, B., Poutanen, J., Svensson, R., Sikora, M., Begelman, M. 1995, ApJ, 449, L13

Tagliaferri, G. 1996, ApJ, 465, 181

Terlevich, R. et al. 1995, MNRAS, 95, 272, 198

Titarchuk, L., Mastichiadis, A. 1994, ApJ, 433, L33

Treves, A., Maraschi, L., Abramowicz, M. 1988, PASP, 100, 427

van der Klis, M. 1995, in X-Ray Binaries, ed. W. Lewin, J. van Paradijs, & van E. van den Heuvel (Cambridge: Cambridge Univ. Press), 252

Van Paradijs, J. 1998, in "The Many Faces of Neutron Stars," Eds. R. Buccheri et al. (Kulwar), in press, astro-ph/9802177

Wanders, I., et al. 1993, A&A, 269, 39

Zdziarski, A., Fabian, A., Nandra, K., Celotti, A., Rees, M., Done, C., Coppi, P., Madejski, G. 1994, MNRAS, 269, L55